

New Challenges: From Physics to Medicine

V. P. Glazkov^a, V. A. Somenkov^a, E. S. Kovalenko^a, and P. A. Borisova^{a,*}

^aNational Research Center Kurchatov Institute, Moscow, 123182 Russia

*e-mail: Borisova_PA@nrcki.ru

Received November 1, 2017

Abstract—The current state of neutron research at the IR-8 reactor is considered and it is shown that the research is focused on two main avenues: comprehensive radiation diagnostics for the sake of those knowledge domains which have not used it before and research of the structure of material under extreme conditions (high pressures, strong magnetic fields, and irradiation). Case studies are given in the areas of materials technology, geology, paleontology, archaeology, and medicine, as well as studies of materials under thermobaric impact and self-radiation. The possibilities of a combination of different experimental techniques are discussed.

Keywords: IR-8 reactor, experimental research

DOI: 10.1134/S1063778818080094

An idea of introducing natural scientific methods into those knowledge domains which have not used them before, espoused by the president of the Kurchatov Institute M. V. Kovalchuk, fully refers to penetrating radiation sources, accelerators, and reactors, which from the very beginning were developed as multipurpose installations. In this regard, studies that are currently under way at the IR-8 reactor are focused on two main trends: the first is comprehensive X-ray, neutron, and gamma-ray diagnostics for the study of the composition and structure of objects for the sake of various knowledge domains (materials technology, geology, archaeology and museum value, paleontology, and medicine), and the second is research of the material structure and phase transitions under extreme conditions (temperature, pressure, irradiation, and strong magnetic fields) for both conventional and for new systems of interest, such as nanoscale carbon, photonic crystals, high-pressure hydrides, and fissile alloys. Accordingly, the equipment for such kind of research is developing as well.

A feature research at the IR-8 is its integrated nature [1–7]. Using the set of techniques available at the reactor (micro and macro diffraction, neutron-radiation analysis, ultra-small-angle spectroscopy, and various types of introscopy, radiography, and tomography), we obtain substantial information on the composition, structure, and structural flaws of objects. For this purpose, various types of reactor radiation (white, filtered, monochromatic, different energies) are used, and, if necessary, the capabilities of the Kurchatov Institute’s synchrotron are engaged as well.

Some of the experiments carried out are briefly described below.

INVESTIGATION OF INTERNAL STRUCTURE OF MATERIALS AND OBJECTS BY NEUTRON INTROSOPY

Materials Technology

Investigations of the structure and structural flaws in poly- and monocrystal superconductors and superconducting targets were carried out. Various types of flaws were detected, in particular, inclusions in superconducting targets (Fig. 1), which are essential for testing the production technology of new-generation superconducting materials. Magnetic inhomogeneities in steels were studied by a refractive contrast imaging technique and it was shown that various phase components (austenite, ferrite, martensite) are radically different in small-angle scattering. Various types of flaws (microporosity, cracks, etc.) in welded steel joints were studied and it was shown that the neutron-optical technique has a significant advantage in comparison with others in terms of rate, sensitivity, minimum flaw size, etc.

High-Tech Products

The internal structural flaws of various types of poly- and monocrystal turbine blades were studied, including blades for new-generation aircraft. Various types of flaws were detected, such as phase inclusions of different orientation, composition inhomogeneity, and underetched residues in cooling channels (Fig. 2). Using a combination of neutron and synchrotron diagnostic techniques, coated particles were investigated. The dimensions and quality of protective shells and the core oxygen composition were determined. In new types of fuel elements with zirconium jacket,

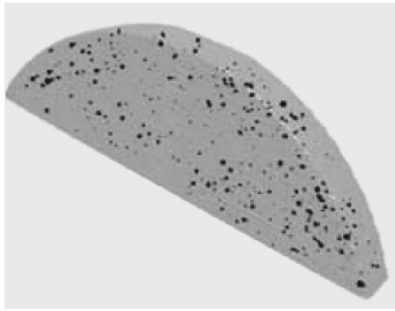


Fig. 1. Three-dimensional reconstruction of a superconducting target according to neutron tomography.

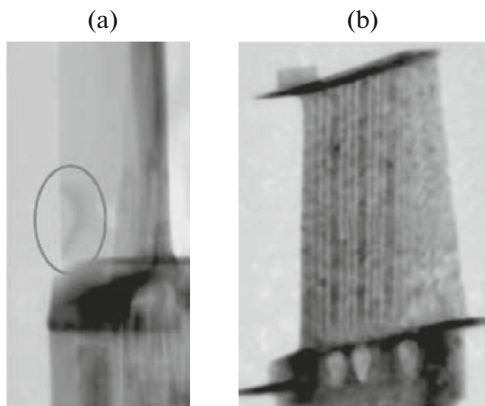


Fig. 2. Flaws of the internal structure of various types of turbine blades: (a) phase inclusion of different orientation (highlighted in by circle); (b) inhomogeneities in channels.

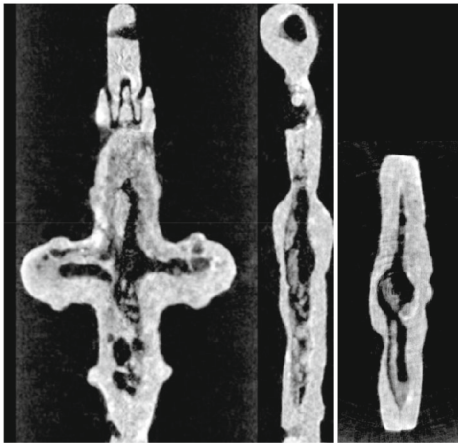


Fig. 3. Neutron tomographic cross sections of the cross.

large-scale inhomogeneities were observed. In addition, real-time microscopy experiments (“neutron cinema”) were conducted to study the processes of crystallization of metals with various bulk transition effects.

Geology

In order to develop methods of detection of large diamonds in rock, kimberlites (Arkhangelsk obalst, Pionerskaya pipe) were studied from a depth of 400 m. It was found that they contain large (up to 1 cm) anti-gorite monocrystals. The minimum sizes of detection were determined on the model samples (diamond/kimberlite) equal to 0.3–0.4 carats. Deep and superdeep drill-hole cores up to a depth of 8000 m were studied and their morphology was determined at different depths. The internal structure of aerosiderites, mesosiderites, and aerolite of various origins (Museum of Nonterrestrial Matter) was investigated and the presence of large- and small-scale inhomogeneities up to the formation of large monocrystals in aerosiderites and mesosiderites was established. A pattern of spherical inclusions, i.e., chondrules, was also evident, indicating an extraterrestrial origin of the object.

Archaeology

By means of comprehensive diagnostics, artifacts of ancient piety were studied: chest-type closed crosses—encolpions of the pre-Mongol period from Soroguzheno and Suzdal Opol’e. It was shown that the cross from Soroguzheno is a cast artifact made of lead-tin bronze, the approximate composition of which (10% Sn and 2% Pb) corresponds to those of the Late Bronze. The presence of internal heterogeneities was established (Fig. 3). The reliquary forms, sizes, and location and the presence of a hydrogen-containing relic in it were determined. On the basis of the existence of similar samples in various collections, considerations were made regarding its possible origin and age.

A study of Donatello’s massive bronze statuettes from the Pushkin State Museum of Fine Arts was carried out, and it was shown that our diagnostic techniques can be used to study relatively large objects (80 cm and more).

Paleontology

Investigation of the internal structure (Figs. 4a, 4b), morphology, and mineralogical and chemical compositions of brachiopods, echinoderms, and other invertebrate objects of ancient fauna was carried. It was shown that a combination of complementary neutron and synchrotron diagnostics significantly exceeds the capabilities of standard X-ray tomography both in terms of contrast and in terms of the object size and thickness. Strontium-containing brachiopods *Rhynchonellida* sp. and *Isortis* sp. were studied and crystal druses were found inside these invertebrates consisting of celestite (strontium sulfate) and aragonite as in most strontium deposits. Trilobites related to different times of the dinosaur era (40–400 million years ago) were also studied. Nerve canals and other features are well

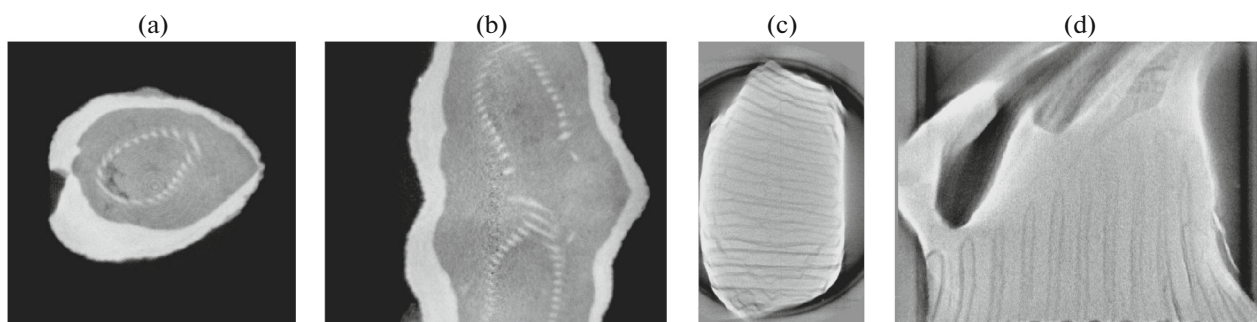


Fig. 4. Internal structure of a fragment of *Kaninospirifer kaninensis* (Licharew, 1943, Urzhum stage, sample 7a/120 no. 4900/79 PIN RAS) according to the results of thermal neutron tomography. The invertebrate's test and hand apparatus are clear in evidence (a, b).

marked out in the image of a mammoth tooth (Figs. 4c, 4d).

Medicine

The structure of the bones of laboratory animals in vitro was studied by techniques of radiography and tomography and numerous bone structural inhomogeneities (Fig. 5), gallstones, and other biominerals were revealed.

Reversible and irreversible phase transitions in the biominerals were detected with elevation of temperature. A study of human bones in health and in disease has been started. The pathological objects demonstrated heterogeneities whose nature is being studied. Low-dose neutron microscopy techniques were developed for medical applications by suppressing part of the fast neutrons and gamma radiation in the beam by means of special filtration of radiation.

The conducted studies illustrate the interpenetration of sciences, including in the areas in which penetrating radiation has not previously been used. Thus, the initial experiments carried out at the IR-8 reactor with the help of comprehensive radiation diagnostics showed significant opportunities for its application in various knowledge domains, revealed the need for active joint cooperation with representatives of various sciences to formulate a promising research program, and contributed to the development of new experimental techniques in respect to the issued challenges.

Investigations of the Structure of Matter and Phase Transitions in Extreme Conditions

Within the scope of the second avenue—the study of the matter under extreme conditions—a number of studies were performed, some of which are described below.

Nanoscale Carbon

The discovery in recent decades of new crystal forms of carbon (including polymer and molecular) and the development of nanoparticle physics make relevant the study of the structural behavior of such nanoscale carbon forms (including amorphous) in a wide range of temperatures and pressures. Carbon is often a reinforcing additive for interacting with metals. It was of interest to study various nanoscale carbon forms as hardening additives in metal-matrix composites (MMC), which are promising materials owing to their properties.

In this regard, over the past few years, the study of the structure and phase transformations of carbon nanomaterials, as well as hardening of iron and aluminum metal matrix composites [8–14], has become an important area of research. The study was carried out on the X-ray powder diffractometer DISK [15]. The effect of pressure on the nanoscale carbon structure at room temperature was studied in situ in sapphire anvil cells. High-pressure sintering was carried out at the Institute for High Pressure Physics (IHPP) of the Russian Academy of Sciences.

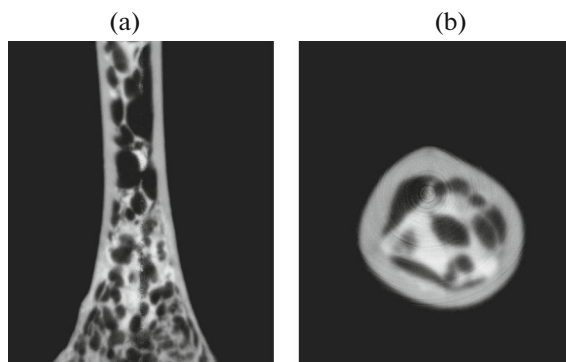


Fig. 5. Longitudinal (a) and transverse (b) tomographic sections of the shinbone sample of *Gallus domesticus* obtained with the help of thermal neutrons.

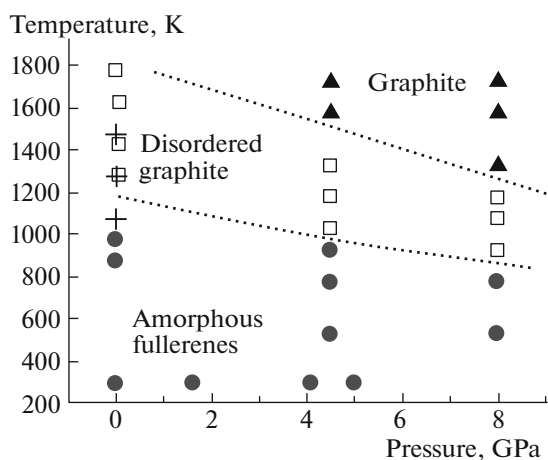


Fig. 6. Nonequilibrium (kinetic) diagram of phase transformations of the amorphous phase of C_{60} fullerenes (crosses—an intermediate phase).

Amorphous Phase of Fullerenes

Neutron diffraction patterns of the virgin crystal fullerenes corresponded to a FCC lattice with constant $a = 14.16 \text{ \AA}$. An amorphous phase of fullerenes was obtained by mechanical milling in an agate activator in a Fritsch mill. The samples thus obtained were subjected to high-temperature (up to 1700°C) stepped annealing in a vacuum annealing furnace for 4 h in each cycle and then cooled to room temperature; they were subjected to pressurization in the sapphire anvils (up to 5 GPa) and sintering in high-pressure toroidal cells (up to 8 GPa).

From the results of experiments, a nonequilibrium (kinetic) diagram of the phase transformations of the amorphous phase of fullerenes C_{60} ($a\text{-}C_{60}$) was constructed (Fig. 6). There are three visible regions: a low-temperature region in which no transformations are detected by diffraction methods and $a\text{-}C_{60}$ continues to exist; a region of medium temperatures in which $a\text{-}C_{60}$ transforms into disordered graphite; and a high-temperature region in which crystalline graphite is formed. With increasing pressure, the temperatures of formation of disordered (amorphous) and crystalline graphite decrease.

In all cases of thermal and pressure effects, $a\text{-}C_{60}$ undergoes transformations that can proceed in two ways: amorphous phase of fullerenes \rightarrow disordered graphite \rightarrow pressurized crystalline graphite or amorphous phase of fullerenes \rightarrow graphene-like intermediate phase \rightarrow disordered graphite \rightarrow unpressurized graphite (turbostratic type). At the same time, in a fullerite, transformations from molecular to atomic (graphite, diamond) phases occur at higher pressures and through a series of molecular polymerization phases. This shows that amorphization lowers the molecule stability and contributes to its collapse, and

high pressures contribute, as a result, to the formation of denser atomic phases.

Structure of Synthetic Photonic Crystals at Various Temperatures and Pressures

Artificial opals are ordered packages of spherical particles of amorphous silicon dioxide ($\alpha\text{-SiO}_2$) which form long-period structures. At the same time, opals at the atomic-scale level have an unordered (amorphous) structure in accordance with various polymorphic silica modifications. It is known that quartz under the influence of temperature and pressure has many polymorphic transformations (α -, β -quartz, tridymite, α -, β -cristobalite with temperature change, coesite and stishovite at high pressures).

Neutron diffraction patterns of the initial opals obtained on the DISK diffractometer [15] clearly reveal diffraction halos, whose positions are retained in the samples with different sizes of globules and correspond to the strongest diffraction lines of the highest temperature silica modification— β -cristobalite. This means that these samples of artificial opals belong to the cristobalite type and form an amorphous (small-crystalline) structure at the atomic-scale level. At the same time, on the ultra-small-angle diffraction pattern near the line corresponding to the primary beam, additional reflections appear corresponding to the ordered lattice of globules. The position of these reflections and the superlattice constant are determined by the size of globules, so that, as the particle size increases, the peaks approach the direction of the primary beam (Fig. 7a).

According to thermogravimetry, when the opals are heated, there is a loss of water at 150°C and a loss of a hydrogenous component at 800°C . In this case, the opals change their color and iridescence [16]. With a further temperature increase to 1500°C , the opals become transparent, and the halo on the neutron diffraction patterns sharpens, indicating the formation of cristobalite glass. At the same time, according to the data of small-angle diffraction, the “superlattice” peaks disappear, indicating the disappearance of the long-range ordering at the globule level, while keeping the short-range ordering at the interatomic level, i.e., the “melting” of the superlattice.

Baric and thermobaric effects were performed with anvil cells up to pressures of 7 GPa and a temperature of up to 500°C . With increasing temperature, the initial amorphous cristobalite opal forms a mixture of amorphous and crystalline coesite, and with a further increase in temperature (to 500°C), single-phase crystalline coesite appears (Fig. 7b). When the pressure is raised to 11 GPa (the region of existence of stishovite), crystallization occurs: crystalline stishovite is formed from amorphous cristobalite, as in the case of coesite. The peculiarity of this transition, in comparison with the formation of stishovite from crystalline silica, is

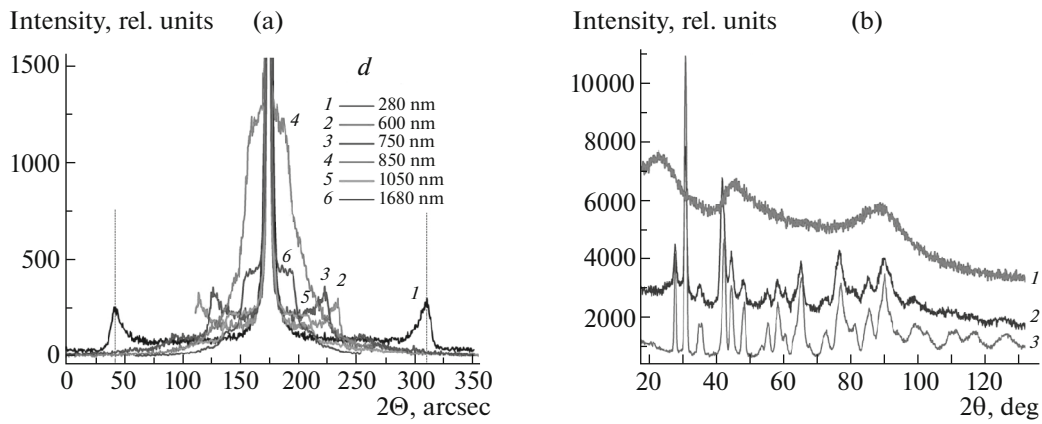


Fig. 7. (a) Neutron small-angle diffraction data ($\lambda = 1.54 \text{ \AA}$); Θ is the angle of crystal rotation. (b) Neutron diffraction patterns of synthetic photonic crystals: (1) initial synthetic photonic crystal; (2) 300°C , 7 GPa, a mixture of amorphous and crystalline coesite; (3) 500°C , 7 GPa, crystalline coesite.

that the region of existence of stishovite expands instead of narrowing with increasing temperature, so that, when the temperature decreases, a coesite and stishovite mixture appears. This is apparently due to the difference in the internal energy of amorphous and crystalline silica.

Pu–Ga ALLOY AGING AT SELF-IRRADIATION

Plutonium has the largest number of polymorphic transformations among metallic elements and forms phases that are stabilized by doping additives. In the aging process of plutonium and its alloys, there is accumulation of radiation defects caused by self-irradiation, which leads to changes in the physical and mechanical properties of the metal and its alloys. These changes are caused by the α decay of plutonium isotopes with the formation of α particles and actinide nuclei. Both the α particles and the actinide nuclei form displacement cascades, and the α particles change to helium atoms and gather in bubbles.

Structural studies of the radiation defects of plutonium and its alloys are aggravated by high toxicity, rapid oxidation, high X-ray absorption capacity, and strong neutron absorption by nuclei of the main isotope ^{239}Pu . Therefore, the research was carried out mainly on a unique sample with a FCC structure prepared on the basis of the isotope ^{242}Pu . To increase the self-irradiation rate, a rapidly decaying isotope ^{238}Pu (1.4 at %) was added. An estimate of the increase in the self-irradiation rate corresponds to a fourfold acceleration compared to samples based on pure plutonium. The experiments were carried out on the DISK diffractometer in successive surveys for 510 calendar days for a $\text{Pu}^{239}\text{–Ga}$ sample and for 3698 calendar days for a $^{242}\text{Pu–Ga}$ one. The maximum equivalent self-irradiation time of the latter was ~ 40 years. The samples were held and examined at room temperature in special containers.

After the maximum holding period of 3698 days, the neutron diffraction pattern had only FCC phase lines coinciding in lattice parameters with the δ phase of the Pu–Ga system. Thus, the self-irradiation of the Pu–Ga alloy samples up to 3698 days (~ 40 equivalent years) did not lead to any noticeable phase transformations. This indicates a very high stability of the δ phase in Pu–Ga alloys. As the holding period (Fig. 8) is increased at the initial stage, there is an increase in mean square atomic displacements in the $^{242}\text{Pu–Ga}$ alloy, which in comparison with the initial samples, have a static nature and reach the maximum level after ~ 800 calendar days (approximately 9 equivalent years). The rise is $\sim 45\%$ of the value for the initial samples. After that, up to ~ 2150 days (approximately 23.5 equivalent years), there is a gradual decrease of $\langle u^2 \rangle$, which approaches a value exceeding the initial value by only $\sim 15\%$.

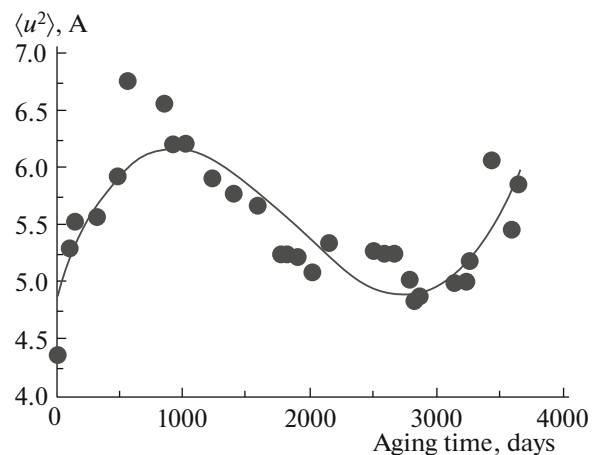


Fig. 8. Variation of the mean square atomic displacement upon aging of the $^{242}\text{Pu–Ga}$ δ -alloy.

Owing to the self-annealing at room temperature, which exceeds the Debye temperature of plutonium ($\Theta_d = 162$ K), the lattice constant of the δ phase at the first stage of self-irradiation increases slightly and decreases at the second stage. Such a nonmonotonic (periodic) character of the variation in the level of crystal lattice damage during self-irradiation and self-annealing of the Pu–Ga alloy was discovered for the first time and can be considered as the main result of this stage of the work [17–19]. It was obtained by direct neutron methods on unique samples for a very long holding period.

CONCLUSIONS

The results show that, in spite of the fact that there are more powerful neutron sources in the country, an original and quite competitive scientific research program based on the new measurement techniques can be developed at the IR-8 reactor within the framework of active research.

ACKNOWLEDGMENTS

V.A. Somenkov is grateful to the Russian Science Foundation (grant no. 16-12-10065) and the Russian Foundation for Basic Research (grant no. 16-02-00755) for partial support of the research.

REFERENCES

1. V. A. Somenkov, A. K. Tklich, and S. Sh. Shil'shtein, *Sov. Tech. Phys.* **36**, 1309 (1991).
2. K. M. Podurets, S. S. Shilstein, and V. A. Somenkov, *Eur. Phys. J. Spec. Top.* **3**, 455 (1993).
3. A. A. Manushkin, D. K. Pogoreliy, K. M. Podurets, et al., *Nucl. Instrum. Methods Phys. Res., Sect. A* **575**, 225 (2007).
4. S. Sh. Shil'shtein and V. A. Somenkov, *Sov. Phys. Crystallogr.* **20**, 670 (1975).
5. V. P. Glazkov, A. A. Kaloyan, E. S. Kovalenko, K. M. Podurets, V. A. Somenkov, and E. V. Yakovenko, *Instrum. Exp. Tech.* **57**, 531 (2014).
6. V. P. Glazkov, E. S. Kovalenko, K. M. Podurets, et al., *Russ. Found. Basic Res. J.*, No. 2 (86), 61 (2015).
7. K. M. Podurets, A. V. Petrenko, V. A. Somenkov, et al., *Tech. Phys.* **39**, 971 (1994).
8. P. A. Borisova, S. S. Agafonov, V. P. Glazkov, et al., *Crystallogr. Rep.* **56**, 1123 (2011).
9. P. A. Borisova, M. S. Blanter, and V. A. Somenkov, *Bull. Russ. Acad. Sci.: Phys.* **78**, 1205 (2014).
10. P. A. Borisova, M. S. Blanter, V. V. Brazhkin, et al., *J. Phys. Chem. Solids* **83**, 104 (2015).
11. V. S. Neverov, P. A. Borisova, A. B. Kukushkin, et al., *J. Non-Cryst. Solids* **427**, 166 (2015).
12. P. A. Borisova, S. S. Agafonov, M. S. Blanter, et al., *Bull. Russ. Acad. Sci.: Phys.* **77**, 1363 (2013).
13. P. A. Borisova, M. S. Blanter, V. V. Brazhkin, et al., *J. Alloys Compd.* **656**, 383 (2016).
14. P. A. Borisova, S. S. Agafonov, M. S. Blanter, et al., *Phys. Solid State* **56**, 199 (2014).
15. V. P. Glazkov, I. V. Naumov, V. A. Somenkov, et al., *Nucl. Instrum. Methods Phys. Res., Sect. A* **264**, 367 (1988).
16. V. A. Somenkov, S. S. Agafonov, V. P. Glazkov, E. S. Kovalenko, and M. N. Shushunov, *Crystallogr. Rep.* **60**, 34 (2015).
17. V. A. Somenkov, M. S. Blanter, V. P. Glazkov, et al., *J. Nucl. Mater.* **413**, 132 (2011).
18. M. S. Blanter, V. P. Glazkov, A. V. Laushkin, V. K. Orlov, V. A. Somenkov, and M. N. Shushunov, *Phys. Met. Metallogr.* **113**, 621 (2012).
19. V. A. Somenkov, V. P. Glazkov, M. S. Blanter, et al., *J. Nucl. Mater.* **452**, 465 (2014).

Translated by A. Kolesesin